Published in final edited form as:
Cancer Lett. 2014 November 28; 354(2): 299–310. doi:10.1016/j.canlet.2014.08.032.

A novel selective multikinase inhibitor of ROCK and MRCK effectively blocks cancer cell migration and invasion

Vijay Pralhad Kale, **Jeremy A. Hengst**, **Dhimant H. Desai**, **Taryn E. Dick**, **Katherine N. Choe**, **Ashley L. Colledge**, **Yoshinori Takahashi**, **Shen-Shu Sung**, **Shantu G. Amin**, and **Jong K. Yun***
Department of Pharmacology, Penn State Hershey College of Medicine, Hershey, PA 17033, USA

Abstract

Two structurally related protein kinase families, the Rho kinases (ROCK) and themyotonic dystrophy kinase-related Cdc42-binding kinases (MRCK) are required for migration and invasion of cancer cells. We hypothesized that simultaneous targeting of these two kinase families might represent a novel therapeutic strategy to block the migration and invasion of metastatic cancers. To this end, we developed DJ4 as a novel small molecule inhibitor of these kinases. DJ4 potently inhibited activities of ROCK and MRCK in an ATP competitive manner. In cellular functional assays, DJ4 treatment significantly blocked stress fiber formation and inhibited migration and invasion of multiple cancer cell lines in a concentration dependent manner. Our results strongly indicate that DJ4 may be further developed as a novel antimetastatic chemotherapeutic agent for multiple cancers.

Keywords

ROCK; MRCK; Multikinase inhibitor; Migration; Stress fibers; Cancer

Introduction

With the advent of targeted therapeutic strategies, major advancements in the treatment of primary tumors have been achieved. However, treatment of metastatic tumors remains a daunting challenge and successful outcomes are limited. Strategies designed to block primary tumor extravasation and/or secondary site invasion have been developed (i.e. matrix metalloproteinase inhibitors; MMPIs); yet these MMPIs have yielded limited clinical success [1]. Hence, the development of new strategies that specifically target the migratory and invasive properties, which are hallmarks, of metastatic cancer cells could be of enormous therapeutic impact [2].

*Corresponding author. Tel.: +001 717 531 1508; fax: +001 717 531 5013. jky1@psu.edu (J.K. Yun).

Conflict of interest
All authors have no conflict of interest.

Appendix: Supplementary Material
Supplementary data to this article can be found online at doi:10.1016/j.canlet.2014.08.032.

The importance and regulation of Rho-associated coiled-coil containing protein kinase (ROCK1 and ROCK2; henceforth referred as ROCK) activity in cancer is being discussed extensively [3,4]. Upregulation of ROCK protein/mRNA expression in various tumor types is positively correlated with tumor stage and progression while it is negatively correlated with overall survival and disease prognosis [5–9]. The role of ROCK in cancer cell migration and invasion has been demonstrated by stable overexpression and knockdown studies of ROCK1 and ROCK2 in various cancer cell lines [10–13]. In contrast to ROCK, the expression of myotonic dystrophy kinase-related Cdc42-binding kinases (MRCKα and MRCKβ; henceforth referred as MRCK) in tumor tissues has not been examined.

Individual cancer cells find their way through the extracellular matrix (ECM) by two distinct mechanisms: amoeboid and mesenchymal modes of migration/invasion [14]. Both modes of migration/invasion require contraction of stress fibers mediated by the phosphorylation of myosin light chain (MLC). ROCK and MRCK have been shown to phosphorylate MLC and have been implicated in regulation of cell contractility [15–17]. The amoeboid mode of invasion is primarily dependent on ROCK activity to generate strong contractile forces and is independent of protease activity [18–20], whereas the mesenchymal mode of cell invasion depends on the activity of MRCK to generate contractile forces [21]. Importantly, studies demonstrate that cancer cells often switch between these two mechanisms when an individual mode of migration/invasion is blocked (reviewed in Refs. [14,22]).

The roles of both ROCK and MRCK in cytoskeletal reorganization during cell migration/invasion have been clearly delineated [16,18,23,24]. Indeed, due to their cooperative regulation of cell migration/invasion [21], we believe simultaneous targeting of ROCK and MRCK would be an effective means of inhibiting cancer cell migration/invasion. In support of this, a recent study demonstrated that simultaneous siRNA mediated knockdown of MRCK and ROCK in MDA-MB-231 cells blocked cancer cell invasion more effectively than knockdown of either kinase alone [25]. The strategy of simultaneous inhibition of both ROCK and MRCK for effective inhibition of metastasis is supported widely [3].

Herein, we report the discovery and development of a novel ATP-competitive multikinase inhibitor, (5*Z*)-2–5-(1H-pyrrolo[2,3-*b*]pyridine-3-ylmethylene)-1,3-thiazol-4(5H)-one (DJ4), that selectively inhibits the activity of ROCK1 and ROCK2 in addition to MRCKα and MRCKβ. We demonstrate the ability of DJ4 to inhibit the migration and invasion of lung, breast, melanoma and pancreatic cancer cell lines, *in vitro*, and have elucidated the molecular mechanism involved in its inhibition of cancer cell migration/invasion.

Materials and methods

Synthesis of DJ4

DJ4 was synthesized as shown in Fig. 1. Detailed synthesis and structural activity studies of DJ4 will be published elsewhere. Briefly, 2-phenethyl thiourea was reacted with anhydrous sodium acetate and ethyl chloroformate to give 2-phenethylimino-thiazolidin-4-ones (compound 1) in quantitative yield. Compound 1 was reacted with 7-azaindole-3-carboxaldehyde, and catalytic amount of piperidine in absolute ethanol for 12 h at 60 °C to give compound 2 (DJ4) in 64% yield. DJ4was obtained as a precipitate from the reaction

mixture, washed with methanol and diethyl ether. Purity was > 90%. ^{1}H NMR (DMSO-D_6) 8.36–8.33 (m, 2H, aromatic), 7.84 (s, 1H, = CH-NH), 7.68 (s, 1H, CH), 7.35–7.2 (m, 6H, aromatic), 3.75 (t, 2H, CH_2, J = 7.5 Hz), 2.94 (t, 2H, CH_2, J = 7.5 Hz).

Cell lines and cell culture

The following cell lines used in this study were obtained from ATCC: NSCLC (A549, CCL-185; H522, CRL-5810; H23, CRL-5800; H2126, CCL-256; H460, HTB-177), melanoma (A375M, CRL-1619), pancreatic cancer (PANC-1, CRL-1469), breast cancer (MDAMB-231, HTB-26) and normal human adult fibroblasts (PCS-201-012). The glioblastoma cell line, U251, was kindly provided by Dr. James Connor (Department of Neurosurgery, Penn State Hershey College of Medicine). Cells were maintained in DMEM or RPMI media (Cellgro, Corning) supplemented with 10% fetal bovine serum (Gibco) and penicillin/streptomycin (Gibco) at 37 °C with 5% CO_2.

Western blot analysis

Cells were lysed in 1× lysis buffer (20 mM Tris pH 7.4, 150 mM NaCl, 1 mM EDTA, 1 mM EGTA, 1% Triton X-100, 2.5 mM sodium pyrophosphate, 1 mM β-glycerophosphate, 1 mM Na_3VO_4) containing Mini-EDTA Free protease inhibitor tablets (Roche). The lysates were centrifuged at 20,000×*g* at 4 °C for 20 min. Total protein was quantified using the bicinchoninic acid (BCA) assay. Equal amounts of total protein were separated on SDS-PAGE gels and expression levels of specific proteins were analyzed by Western blot. The following antibodies were employed: pMYPT1 (Thr696, Millipore), MYPT1 (Upstate), pMLC (Ser19, Cell Signaling), ROCK1 (Abcam), ROCK2 (Abcam), β-actin (Cell Signaling), and GAPDH (Cell Signaling).

Protein expression in human lung tumors

To analyze expression of ROCK1/2 and pMYPT1 in lung tumors, tissue samples were obtained from the Penn State Hershey tissue bank with IRB approval. Total protein was isolated and quantified using the Nucleospin RNA/Protein Isolation Kit (Machery Nagel) per manufacturer's instructions. Western blot analysis of ROCK1/2 and pMYPT1 (Thr696) protein expression was performed as stated above. MYPT1 is known to be phosphorylated at Thr853 (myosin-binding regulatory phosphorylation site) [26] by ROCK while at Thr696 (inhibitory phosphorylation site) by both ROCK and MRCK. In this experiment, phosphorylation status of Thr696 was investigated to study total phosphorylation of MYPT1 at inhibitory site.

Kinase activity assays

Cell-free (biochemical) activity assays—Recombinant ROCK1 (9.48 nM) or ROCK2 (8.26 nM; Invitrogen) was incubated in the presence of different concentrations of DJ4 or DMSO in ROCK assay buffer (50 mM Tris pH 7.4, 0.1 mM EGTA, 0.001% β-mercaptoethanol and 10 mM magnesium acetate) at room temperature (RT) for 10 min. MRCKα, MRCKβ, PAK1 and DMPK (2 ng/μL; Invitrogen) assays were performed in assay buffer containing 25mMHEPES (pH 7.5), 10 mM $MgCl_2$, 0.5 mM EGTA, 0.5 mM Na_3VO_4, 5 mM β-glycerophosphate, 2.5mM DTT and 0.01% Triton X-100. Recombinant MYPT1 (20

ng/μL; Millipore) and ATP (5 μM) were added to initiate the reaction. The reaction was incubated at 30 °C for 20 min. Known ROCK inhibitors Y27632 (Selleck Chemicals LLC) and hydroxyfasudil (Santa Cruz Biotechnology) were used at 1 μM concentration as positive controls. Samples without respective kinases were used as negative controls. Phosphorylation of MYPT1 was determined by Western blot analysis using anti-pMYPT1 (Thr696) antibodies. Competitive binding assays for ROCK1 and MRCKβ kinases were performed at 5, 25, 50 μM concentrations of ATP while keeping all other conditions similar.

Activity assays in non-small cell lung cancer (NSCLC) cell lines—A549 cells were treated with different concentrations of DJ4 for 24 h. In an independent experiment, H2126, H23, H460 and H522 cells were treated with 5 μM DJ4 for 24 h. Cell lysates were prepared and protein was quantified per procedure detailed in the 'Western blot analysis' section. Equal quantities of total protein were incubated in the presence of ATP (25 μM) with or without recombinant MYPT1 (Millipore) at 30 °C for 25 min. Phosphorylation of MYPT1was determined by Western blot analysis using anti-pMYPT1 (Thr696) antibodies.

DJ4 mediated inhibition of endogenous ROCK/MRCK activity—A549 cells were treated with DMSO or DJ4 for 24 h. Cell lysates were prepared and protein was quantified per procedure detailed in the 'Western blot analysis' section. Equal amounts of total protein were separated on SDS-PAGE gels and the levels of pMYPT1 (Thr696, Millipore) and pMLC (Ser19, Cell Signaling) were determined by Western blot analysis. To detect phosphorylation of MYPT1 in MDA-MB-231 (breast cancer), cells were treated with the indicated concentration of DJ4 for 24 h and Western blot analysis was performed using anti-pMYPT1 (Thr696) antibodies.

Fluorescent microscopy of stress fibers—A549 cells and human adult fibroblasts were plated in DMEM medium containing 10% FBS on glass bottom plates (MatTek Corporation). After treatment with DJ4 or DMSO for 1 h, cells were washed and fixed with 4% paraformaldehyde (alcoholfree) in PBS for 10 min at RT. Fixed cells were washed with PBS and permeabilized with 0.5% Triton X-100 in PBS for 10 min at RT. Cells were further washed with PBS and stained with 1 μM DAPI (to visualize nucleus; Invitrogen) and 1 U rhodaminephalloidin (to visualize actin filaments; Invitrogen) for 1 h at RT. Subsequently, cells were washed with PBS three times for 30min each, and images were captured (600×) using an inverted fluorescent microscope (Nikon Eclipse TE2000-S). Images were merged using Photoshop (Adobe Inc.).

Confocal microscopy—Human adult fibroblasts and H522 cells were treated with 5 μM DJ4 for 8 h and 3.5 h, respectively, and stained with rhodamine-phalloidin (actin filaments) and DAPI (nuclei). Images of stress fibers (400×) were captured by confocal microscopy (SP8, Leica). The images were processed using Imaris software (Bitplane scientific software).

Fluorescent microscopy of GFP tubulin expressing U251 cells—U251 glioblastoma cells were stably transfected with EGFP-Tubulin (Clontech; generous gift of Dr. Chris Yengo, Penn State Hershey College of Medicine) by G418 selection. U251 cells were plated in DMEM medium containing 10% FBS on glass bottom plates (MatTek

corporation). After treatment with DJ4 or DMSO for 4 h, cells were counterstained with DAPI to visualize nuclei and images were captured (600×) using an inverted fluorescent microscope (Nikon Eclipse TE2000-S). Images were merged using Photoshop (Adobe Inc.).

Migration and invasion assays

Scratch assay—H522 (lung), PANC-1 (pancreas), MDA-MB-231 (breast), and A375M (melanoma) cancer cells were seeded in 6-well culture plates (Falcon) and grown in DMEM with 10% FBS (complete media) until confluent. Cells were pre-treated for 24 h with DJ4 or DMSO in complete media. After 24 h uniform vertical and horizontal scratches were made through the cell monolayers and monolayers were washed gently, with 1× PBS, to remove dislodged cells. Cells were then allowed to migrate in the presence of either DJ4 or DMSO in complete media for 6–7 h (MDA-MB-231 and PANC-1) and 11–12 h (A375M). Images were captured at the beginning and end of the experiment and the widths of the scratched monolayers were measured at twelve different locations with AxioVision software (AxioVision Inc.). The mean percentage of migration of each treatment was calculated and normalized to that of vehicle (DMSO) control. Data were analyzed by one-way ANOVA and Dunnett's multiple comparisons post-test.

Alternatively, to demonstrate that the migration inhibition effects of DJ4 are independent of growth inhibition, confluent monolayer A549 cells, cultured in complete media, were pre-treated with DJ4, 30 μM Y-27632 or DMSO for 24 h. After treatment, uniform vertical and horizontal scratches were made through the cell monolayer. Cells were washed and allowed to migrate in complete media in the absence of treatments for 9 h. Images were captured and analyzed as above.

Transwell invasion assays (Boyden chamber)—For invasion assays, MDA-MB-231 or A375M cells were serum starved for 17 h in serum-free DMEM medium. After 17 h, 5×10^4 cells were transferred onto Matrigel pre-coated invasion inserts (BD Biocoat) and were allowed to attach for 4 h in serum-free medium. Upon attachment, media containing 20% FBS were added to the bottom chamber, cells were treated with DJ4 or DMSO and allowed to invade for 48 h. At the end of the treatment period, the cells that had invaded to the opposite side of the Transwell membrane were washed with PBS and fixed in chilled 100% methanol for 5–10 min and air dried. Cells were stained with 0.5% crystal violet for 8–10 min, thoroughly washed and dried. Images were captured at 40× magnification. The crystal violet dye from the cells was dissolved in 10% glacial acetic acid for 15 min. Optical density (OD) was measured at 540 nm wavelength by a spectrophotometer and relative % invasion was calculated. All procedures were similar in A549 lung cancer cell line except 2.5×10^4 cells were plated and at the end of assay cells were manually counted.

Time-lapse microscopy and cell tracking studies—To determine the rate of cell migration, cells were monitored by time-lapse microscopy over a period of 21–24 h. Briefly, A549 and MDA-MB-231 cells (2.0×10^4 and 1.0×10^4 cells per well respectively) were plated on 4-well glass bottomed chamber slides (Lab-Tek Chamber Slide, Nunc) in DMEM medium containing 10% FBS. Cells were pretreated with either DMSO or 5 μM DJ4 for 3 h prior to capturing images. Images of the cells (200×) were captured (IX81 microscope;

Olympus) at 10 min intervals for 21–24 h at 37 °C in a 5% CO_2 environment. Cells were tracked at four different locations in each well and the rate of migration was determined using NIS-Elements Viewer (Nikon) and ImageJ (NIH, with MTrackJ plugin) software. Significance of differences in the migration rate (nm/sec) between vehicle control and DJ4 treated cells was determined by two-tailed unpaired t-test in GraphPad Prism 5 (version 5.1, GraphPad Software, Inc.).

Flow cytometry—To determine the number of live and dead cells after DJ4 treatment, A549 cells were treated either with DJ4 or DMSO (vehicle) for 24 h. Cells were trypsinized with 0.05% trypsin for 1 min, trypsin was neutralized by the addition of DMEM medium containing 10% FBS and cells were collected by centrifugation at 500×*g* for 5 min. Collected cells were stained with calcein and ethidium homodimer for 15–20 min as per manufacturer's instructions (Live/Dead Viability/cytotoxicity kit for mammalian cells, Molecular Probes). Stained cells were analyzed by BD FACS Calibur (BD Biosciences) to determine the percentage of live and dead cells. As a positive control for cell death, cells were treated with absolute methanol for 10 min.

MTT assays—A549 cells (2.0×10^4) were seeded into 96-well plates. Cells were treated with DMSO or DJ4 for 24 h. Cells were then incubated with 100 μg of MTT (3-(4,5-dimethylthiazol-2-yl)-2,5-diphenyltetrazolium bromide; Sigma) at 37 °C for 3 h to develop formazan crystals. Crystals were dissolved in 100 μL DMSO. Absorbances at 570 nm and 630 nm (background) were recorded.

Results

ROCK1 and ROCK2 are overexpressed in human lung tumors

As mentioned above, several previous reports have demonstrated that ROCK is over-expressed in a variety of human tumor tissues [5–9]. To date, however, ROCK expression in lung tumor tissues has not been examined. Given the role of ROCK in migration and the inherent nature of lung cancer to become metastatic, as well as the inherent nature of cancers to metastasize to the lung, we were interested in determining whether ROCK was overexpressed in histopathologically graded metastatic lung tumor tissues. Tissues were examined for the expression of ROCK1, ROCK2 and ROCK/MRCK activity (as determined by the presence of MYPT1 phosphorylation at Thr696) in tumor tissues relative to that of normal adjacent tissues from the same patient, by Western blot analysis. The results demonstrated that ROCK1 and/or ROCK2 were consistently overexpressed in the tumor tissues (Fig. 2) relative to normal adjacent tissues. We also detected elevated levels of MYPT1 phosphorylation (ROCK/MRCK activity) in 6 of 7 samples consistent with the observed elevation of ROCK expression. Together, these data indicate that ROCK (either ROCK1 or ROCK 2) protein expression and catalytic activity are consistently elevated in tumor tissues bearing metastatic histopathological grades regardless of site of tumor origin.

DJ4 is a selective, ATP-competitive inhibitor of ROCK1/2 and MRCKα/β

Recently, we developed a series of novel isothiocyanate derivatives and, from these studies, identified DJ4 as a potent inhibitor of ROCK1 and ROCK2 (manuscript in preparation).

ROCK1 and ROCK2 are part of a larger, structurally related family of protein kinases that includes the family prototype, myotonic-dystrophy protein kinase (DMPK), as well as MRCKα and β [23]. Given their sequence similarity, we investigated whether DJ4 was able to selectively inhibit the kinase activity of these related kinases. As shown in Fig. 3A, DJ4 dose-dependently inhibited the phosphorylation of recombinant MYPT1(Thr696) by recombinant ROCK1 and ROCK2 with IC50s of approximately 5 and 50 nM respectively. Similarly, DJ4 dosedependently inhibited the kinase activity of MRCKα and MRCKβ with IC50s of approximately 10 and 100 nM respectively, whereas PAK1 and DMPK were minimally inhibited, if at all, at those concentrations (Fig. 3B). The known selective ROCK inhibitors Y27632 and hydroxyfasudil, at 1 μM concentrations, inhibited the kinase activity of ROCK1 and ROCK2 effectively while sparing MRCKα/β, PAK1 and DMPK.

To better understand the inhibitory mechanism of DJ4, we initially performed docking studies of DJ4 onto the X-ray crystal structure of ROCK1 (2ETR.PDB), ROCK2 (2F2U.PDB), and MRCKβ (3TKU.PDB) using the docking program GLIDE (Schrodinger LLC). These docking studies predict that DJ4 acts as an ATP competitive inhibitor of these kinases (data not shown). To confirm the modeling predictions, we performed *in vitro* ROCK1 kinase activity assays at various concentrations of DJ4 in the presence of increasing concentrations of ATP. We found that increasing concentrations of ATP abrogated the inhibitory effects of DJ4 (Fig. 3C). Similar results were obtained in MRCKβ kinase activity assays (Supplementary Fig. S1). Together, these data suggest that DJ4 is indeed an ATP competitive inhibitor of the ROCK and MRCK kinase families.

DJ4 is cell permeable and active in cells

To determine whether DJ4 is cell permeable and can inhibit the kinase activity of ROCK/MRCK in cells, we treated A549 cells with increasing concentrations of DJ4 (i.e. 2.5 μM and 5 μM) for 24 h. Subsequently, cells were extensively washed, whole cell lysates were prepared and the kinase activity of ROCK/MRCK was assessed by monitoring the phosphorylation of exogenous recombinant MYPT1 peptide by Western blot analysis. As shown in Fig. 3D, the phosphorylation of MYPT1 peptide is effectively blocked in cell lysates prepared from cells treated with DJ4 indicating that DJ4 is cell permeable and is an effective inhibitor of ROCK/MRCK activity in cells. When we further examined the inhibitory activity of DJ4 in several other NSCLC cell lines, we observed that DJ4 (5 μM) effectively blocked recombinant MYPT1 phosphorylation in all the cell lines tested with varying potency (Supplementary Fig. S2).

To further determine whether DJ4 is effective at blocking the phosphorylation of the endogenous ROCK/MRCK substrate proteins MYPT1 and MLC, A549 cells were treated with increasing concentrations of DJ4 for 24 h and the phosphorylation of endogenous MYPT1 and MLC were examined by Western blot analysis. As shown in Fig. 3E, DJ4 treatment effectively inhibited the phosphorylation of both endogenous MYPT1 and endogenous MLC indicating that the DJ4 is cell permeable and active in the intracellular microenvironment. The residual phosphorylation of MLC in the presence of DJ4 likely represents phosphorylation of MLC by other protein kinases (i.e. myosin light chain kinase, PAK1 etc). Knockdown of MRCK by using MRCK-specific siRNA and inhibition of ROCK

by Y27632 have both been shown previously to effectively reduce phosphorylation of MYPT1 (Thr696) and MLC (Thr18/Ser19) [21]. Similarly, DJ4 also reduced phosphorylation of endogenous MYPT1 (Thr696) in MDA-MB-231 breast cancer cells after 24 h treatment (Fig. 3F).

DJ4 reduces stress fiber formation

Stress fibers, which are primarily composed of filamentous (F)-actin and myosin II, are required for the contractile processes involved in cell migration. Previous studies have demonstrated that ROCK1 siRNA inhibited stress fiber formation [27]. With the hypothesis that DJ4 inhibits stress fiber formation by blocking the activity of ROCK and MRCK, we next visualized stress fibers by staining for F-actin using rhodamine-phalloidin. After 1 h of treatment with DJ4, stress fiber formation was dramatically reduced in both A549 cells and normal adult human fibroblasts (Fig. 4A). As a positive control for inhibition of stress fiber formation in cells, we also treated fibroblasts with blebbistatin (a myosin II ATPase inhibitor; 30 μM). Alternatively for confocal microscopy, H522 cells and human adult fibroblasts were treated with 5 μM DJ4 for 3.5 h and 8 h respectively, fixed in 4% paraformaldehyde and stained with rhodaminephalloidin (for F-actin) and counterstained with DAPI (to visualize nuclei). By confocal microscopy, stress fibers were prominently observed in DMSO treated fibroblasts and H522 control cells (Fig. 4B), whereas DJ4 treatment noticeably reduced stress fibers in both cell lines (Fig. 4B; Supplementary Fig. S3, Supplementary Movies S1 and S2). In contrast, DJ4 did not affect the formation/stability of microtubules (Fig. 4C). Together, these results suggest that DJ4 inhibits stress fiber formation (F-actin) via inhibition of ROCK/MRCK activity.

DJ4 inhibits migration and invasion of cancer cells

Given that phosphorylation of MYPT1 and MLC regulates cell contractility and stress fiber formation and that these proteins are required for cellular migration and invasion, we next examined the ability of DJ4 to inhibit these processes. To this end, confluent monolayers of human lung (H522), breast (MDA-MB-231), and pancreatic (PANC-1) cancer cell lines were treated for 24 h with either 2.5 μM DJ4 or DMSO and migration was examined by performing scratch assays. H522, MDA-MB-231 and PANC-1 cells treated with DJ4 (2.5 μM) migrated only 26, 15 and 5% of their respective DMSO treated controls (Fig. 5A). While in the presence of 5 μM DJ4, H522, MDA-MB-231 and PANC-1 cells migrated only 12, 2 and 3% compared to their controls, respectively. Similar results were obtained with melanoma cell line A375M (Fig. 5B) except that the concentration of DJ4 required to significantly inhibit migration of A375M cells was almost 10 fold less (0.25 μM) than the other cell lines tested.

In the scratch assay experiments conducted above (Fig. 5A and B), migration was allowed to proceed in the presence of DJ4. Although DJ4 effectively inhibited migration under these conditions, we cannot preclude the possibility that a blockage of cell proliferation, mediated by DJ4, is contributing to the migration inhibitory effects. To eliminate this possibility, we pretreated A549 cells with DJ4, Y-27632 (a known ROCK inhibitor) or DMSO for 24 h. After pretreatment, the cell monolayers were scratched, extensively washed and cells were allowed to migrate in the absence of treatment for 9 h. Because the normal doubling time of

A549 cells is approximately 24 h, allowing the cells to migrate for only 9 h eliminates the possibility that inhibition of wound closure in the DJ4 treated cells was a result of inhibition of cell proliferation. As shown in Fig. 5C, DMSO treated cells migrate into the wounded area during the 9 h window of migration. While some cell division may have occurred during this window, the majority of wound closure is likely to be the result of actual cell migration. Similarly, substantial wound closure occurred in response to Y-27632 (30 μM) treatment. In contrast, DJ4 effectively blocked wound closure at both 2.5 μM and 5.0 μM concentrations. These results suggest that the cell migration inhibitory effect of DJ4 is independent of its inhibitory effect on cell proliferation. Quantitation of the results of Fig. 5C revealed that DJ4 treated A549 cells migrated significantly less (44% at 2.5 μM and 13% at 5.0 μM) relative to DMSO controls (Fig. 5D). In fact, DJ4 at 2.5 μM inhibited A549 cell migration to a greater extent than Y-27632 at 30 μM indicating that simultaneous inhibition of ROCK and MRCK by DJ4 inhibits cancer cell migration more effectively than ROCK inhibition alone.

To examine the potential of DJ4 to inhibit cancer cell invasion, we conducted invasion assays by allowing MDA-MB-231 cells to invade Matrigel coated Transwell membranes in the presence or absence of DJ4 (5 μM). Consistent with the data obtained in scratch assays, in the presence of 5.0 μMDJ4, invasion of MDA-MB-231 cells through Matrigel was reduced to 30% of DMSO treated controls (Fig. 5E and F). Similar results were obtained in A375M (melanoma) and A549 (NSCLC) cells (Supplementary Fig. S4).

To visualize and quantify the inhibition of cell migration over a period of time (migration rate), we employed time-lapse microscopy of treated and untreated A549 and MDA-MB-231 cells over a 24 h time period. Using single cell tracking techniques we observed that DJ4 (5 μM) treatment reduced the migration rate of A549 and MDA-MB-231 cells by 2.7 and 5.5 fold, respectively, compared to the DMSO treated control cells (Fig. 6A and B; Supplementary Movies S3–S6). The representative single cell tracking of A549 and MDA-MB-231 cells over a 21–24 h time period is shown in Fig. 6C. Together, these results clearly demonstrate that DJ4 treatment inhibits migration/invasion of cancer cells, most likely by blocking ROCK/MRCK activities. Consistent with these observations, the combination of siRNA mediated MRCKα/β knockdown and inhibition of ROCK by Y27632 has been reported to have a more pronounced inhibitory effect on invasion of MDA-MB-231 cells in 3D Matrigel compared to inhibition of either kinase alone [25].

Inhibition of lung cancer cell migration by DJ4 is independent of cell death

While the effects of DJ4 on cell migration/invasion are consistent with the known roles of ROCK and MRCK, it is possible that the migration inhibitory effect of DJ4 is an indirect effect attributed to cell death induction. To examine this possibility, confluent A549 cells were treated with different concentrations of DJ4 for 24 h and MTT assays were performed. Cell viability was reduced by 14% in response to 5 μM DJ4 treatment (Fig. 7A) indicating that DJ4 at this concentration does induce moderate levels of cell death. These results were confirmed by flow cytometry analysis of calcein (live cells) and ethidium homodimer (dead cells) stained cells (Fig. 7B). However, the low level of cell death induction is contrasted to the near complete inhibition of cell migration at this concentration as observed in Figs 5C

and D and 6A–C. Together, these results demonstrate that, at the concentrations and treatment durations employed in these studies, DJ4 does not significantly induce cell death in A549 cells. Thus, the effects of DJ4 on cell migration/ invasion can be attributed to inhibition of ROCK/MRCK signaling.

Discussion

Treatment of metastatic cancers is one of the biggest challenges facing oncologists. Therapeutic strategies such as blocking ECM degradation to prevent metastasis have been envisioned (i.e. MMP inhibitors). However, these strategies have been disappointing in the clinical setting. ROCK specific inhibitors have been in the development without much significant progress [28–30]. ROCK and MRCK are known to cooperatively regulate the formation of stress fibers, cytoskeleton remodeling and establishing front–rear polarity by transducing extracellular stimuli through phosphorylation of multiple intracellular targets (Fig. 8; [24,31,32]). As these processes are required for cancer cell migration/invasion, we hypothesized that simultaneous targeting of ROCK and MRCK would be an effective therapeutic strategy for blocking cancer cell metastasis (i.e. migration/invasion). Hence, we developed a class of novel isothiocyanate derivatives as ROCK and MRCK inhibitors (manuscript in preparation). Evaluation of those compounds identified DJ4 as one of the most potent inhibitors of both ROCK and MRCK. Herein, we have extended these studies to demonstrate that DJ4 is an ATP competitive multikinase inhibitor that inhibits ROCK1, ROCK2, MRCKα and MRCKβ without inhibition of DMPK (another member of the DMPK protein kinase family). Our results presented herein clearly demonstrate that DJ4 potently blocks cancer cell migration and invasion *in vitro*, warranting further evaluation of DJ4 in an *in vivo* model of metastasis. In-cell kinase activity assay and other preliminary data (unpublished) indicate that certain cell lines, such as H23 and H460, are relatively less responsive to DJ4. One possible explanation for this observation is that H23 and H460 cells are less migratory than the other cell lines employed in this study. We employed phosphorylation of MYPT1 at Thr696 as a marker of ROCK/ MRCK activity in our assays. It is possible that the observed phosphorylation of MYPT arises from other MYPT1 protein kinases which are insensitive to DJ4. Further investigations to unearth the molecular mechanisms involved in differential sensitivity toward DJ4 treatment in these cell lines are currently ongoing.

The anti-migration and anti-invasion effects of ROCK-selective inhibitors like Y-27632 [12,33–35], fasudil [36–38], RKI-1447 [39], Wf-536 [40] and OXA-06 [13] have been reported previously in various cancer cells/*in vivo* models. As discussed above, ROCK and MRCK cooperatively regulate cancer cell migration [21] and their simultaneous siRNA mediated inhibition proved to be a better strategy to curb migration/invasion of amoeboid and mesenchymal type cells than inhibition of either kinase alone [21,25].

Recent studies also demonstrate that, in some cases, cancers of epithelial origin will cooperatively migrate with tumor associated fibroblasts in a process termed “collective migration”. In collective cell migration, the stromal fibroblasts rely on ROCK to invade the ECM and pave the way for carcinoma cells, relying on MRCK to follow the tracks generated by the stromal fibroblasts [41]. Combined inhibition of ROCK and MRCK, using

DJ4, may also effectively inhibit collective migration of stromal fibroblasts (ROCK dependent) and carcinoma cells (MRCK dependent) [41]. Hence, as a potent inhibitor of both ROCK and MRCK activity, we believe that DJ4 may hold promise as an effective strategy to inhibit cancer cell metastasis across a broad spectrum of cancer types.

Due to the inherent nature of lung cancer to become metastatic as well as the inherent nature of cancers to metastasize to the lung, we chose to analyze the expression of ROCK protein in human patient lung tumors. While the frequent overexpression of ROCK protein/mRNA has been reported in renal cell carcinoma [5], testicular germ cell tumors [6,9], urinary bladder cancer [8], breast cancer [11,12] and hepatocellular carcinoma [10], the expression of ROCK in human lung tumors has not been reported. To fill this gap, we analyzed the expression of ROCK and phosphorylation status of its substrate (pMYPT1) in histopathologically graded metastatic lung tumor tissues. We observed upregulation of either ROCK1 and/or ROCK2 in tumor tissues compared to adjacent normal tissue from the same patient. Increased phosphorylation of MYPT1 (Thr696) indicates that not only is the expression of ROCK1/2 protein upregulated, but their activity is also increased inmetastatic tumors. However, we should note that MRCKα and MRCKβ are also known to phosphorylate MYPT1 at Thr696. We have not yet analyzed the expression of the MRCK kinases in lung tumor tissues. Thus, it is possible that the observed increase in pMYPT1 (observed in Fig. 2) may also arise from MRCK over-expression. Additionally, apart from upregulation of ROCK/MRCK mRNA or protein, increased activity of ROCK/MRCK may be due to increased signaling originating from RhoA and/or Cdc42, the activators of ROCK and MRCK respectively. Consistent with this, RhoA has been shown to be overexpressed in lung, breast and colon tumors [42,43].

Together, these findings suggest that ROCK and/or MRCK mediated signaling may play an important role in the processes of lung cancer metastasis as well as the process of other cancers metastasizing to the lung. These data combined with the observation that DJ4 potently inhibits the migration/invasion of multiple cancer cell lines further suggest that a mouse metastatic cancer model system would be an appropriate model for further evaluation of the *in vivo* effectiveness of DJ4 or its subsequent analogs. To these ends further optimization of the DJ4 chemotype and *in vivo* evaluation of the effectiveness of DJ4/analogs are ongoing in our laboratory.

Supplementary Material

Refer to Web version on PubMed Central for supplementary material.

Acknowledgments

We thank the Department of Pharmacology, Penn State Hershey Cancer Institute, NCI (Contract # NO2-CB-81013-74 (SGA)) and Jake Gittlen Cancer Research Foundation for financial support (JKY) for this project. Authors are also grateful to Dr. H.G. Wang for providing the facility and Jacob Serfass for his kind technical help during time-lapse microscopy studies. Confocal images were generated at the Microscopy Imaging Facility, Section of Research Resources, Penn State Hershey College of Medicine. Authors are thankful to Dr. Thomas Abraham for his help during confocal imaging. We also thank Dr. Chris Yengo and Dr. James Connor for their gift of the EGFP-Tubulin construct and U251 cell lines respectively.

References

1. Coussens LM, Fingleton B, Matrisian LM. Matrix metalloproteinase inhibitors and cancer: trials and tribulations. Science. 2002; 295:2387–2392. [PubMed: 11923519]
2. Hanahan D, Weinberg RA. Hallmarks of cancer: the next generation. Cell. 2011; 144:646–674. [PubMed: 21376230]
3. Rath N, Olson MF. Rho-associated kinases in tumorigenesis: re-considering ROCK inhibition for cancer therapy. EMBO Rep. 2012; 13:900–908. [PubMed: 22964758]
4. Morgan-Fisher M, Wewer UM, Yoneda A. Regulation of ROCK activity in cancer. J. Histochem. Cytochem. 2013; 61:185–198. [PubMed: 23204112]
5. Abe H, Kamai T, Tsujii T, Nakamura F, Mashidori T, Mizuno T, et al. Possible role of the RhoC/ROCK pathway in progression of clear cell renal cell carcinoma. Biomed. Res. 2008; 29:155–161. [PubMed: 18614849]
6. Kamai T, Arai K, Sumi S, Tsujii T, Honda M, Yamanishi T, et al. The rho/rho-kinase pathway is involved in the progression of testicular germ cell tumour. BJU Int. 2002; 89:449–453. [PubMed: 11872041]
7. Kamai T, Arai K, Tsujii T, Honda M, Yoshida K. Overexpression of RhoA mRNA is associated with advanced stage in testicular germ cell tumour. BJU Int. 2001; 87:227–231. [PubMed: 11167647]
8. Kamai T, Tsujii T, Arai K, Takagi K, Asami H, Ito Y, et al. Significant association of Rho/ROCK pathway with invasion and metastasis of bladder cancer. Clin. Cancer Res. 2003; 9:2632–2641. [PubMed: 12855641]
9. Kamai T, Yamanishi T, Shirataki H, Takagi K, Asami H, Ito Y, et al. Overexpression of RhoA, Rac1, and Cdc42 GTPases is associated with progression in testicular cancer. Clin. Cancer Res. 2004; 10:4799–4805. [PubMed: 15269155]
10. Wong CC-L, Wong C-M, Tung EK-K, Man K, Ng IO-L. Rho-kinase 2 is frequently overexpressed in hepatocellular carcinoma and involved in tumor invasion. Hepatology. 2009; 49:1583–1594. [PubMed: 19205033]
11. Lane J, Martin TA, Watkins G, Mansel RE, Jiang WG. The expression and prognostic value of ROCK I and ROCK II and their role in human breast cancer. Int. J. Oncol. 2008; 33:585–593. [PubMed: 18695890]
12. Liu S, Goldstein RH, Scepansky EM, Rosenblatt M. Inhibition of rho-associated kinase signaling prevents breast cancer metastasis to human bone. Cancer Res. 2009; 69:8742–8751. [PubMed: 19887617]
13. Vigil D, Kim TY, Plachco A, Garton AJ, Castaldo L, Pachter JA, et al. ROCK1 and ROCK2 are required for non-small cell lung cancer anchorage-independent growth and invasion. Cancer Res. 2012; 72:5338–5347. [PubMed: 22942252]
14. Friedl P, Alexander S. Cancer invasion and the microenvironment: plasticity and reciprocity. Cell. 2011; 147:992–1009. [PubMed: 22118458]
15. Vicente-Manzanares M, Ma X, Adelstein RS, Horwitz AR. Non-musclemyosin II takes centre stage in cell adhesion and migration. Nat. Rev. Mol. Cell Biol. 2009; 10:778–790. [PubMed: 19851336]
16. Zhao Z-S, Manser E. PAK and other Rho-associated kinases – effectors with surprisingly diverse mechanisms of regulation. Biochem. J. 2005; 386:201–214. [PubMed: 15548136]
17. Ishizaki T, Naito M, Fujisawa K, Maekawa M, Watanabe N, Saito Y, et al. p160ROCK, a Rho-associated coiled-coil forming protein kinase, works downstream of Rho and induces focal adhesions. FEBS Lett. 1997; 404:118–124. [PubMed: 9119047]
18. Sahai E, Marshall CJ. Differing modes of tumour cell invasion have distinct requirements for Rho/ROCK signalling and extracellular proteolysis. Nat. Cell Biol. 2003; 5:711–719. [PubMed: 12844144]
19. Kosla J, Pankova D, Plachy J, Tolde O, Bicanova K, Dvorak M, et al. Metastasis of aggressive amoeboid sarcoma cells is dependent on Rho/ROCK/MLC signaling. Cell Commun. Signal. 2013; 11:51. [PubMed: 23899007]

20. Wyckoff JB, Pinner SE, Gschmeissner S, Condeelis JS, Sahai E. ROCK- and myosin-dependent matrix deformation enables protease-independent tumor-cell invasion in vivo. Curr. Biol. 2006; 16:1515–1523. [PubMed: 16890527]
21. Wilkinson S, Paterson HF, Marshall CJ. Cdc42-MRCK and Rho-ROCK signalling cooperate in myosin phosphorylation and cell invasion. Nat. Cell Biol. 2005; 7:255–261. [PubMed: 15723050]
22. Wolf K, Mazo I, Leung H, Engelke K, von Andrian UH, Deryugina EI, et al. Compensation mechanism in tumor cell migration: mesenchymal-amoeboid transition after blocking of pericellular proteolysis. J. Cell Biol. 2003; 160:267–277. [PubMed: 12527751]
23. Riento K, Ridley AJ. Rocks: multifunctional kinases in cell behaviour. Nat. Rev. Mol. Cell Biol. 2003; 4:446–456. [PubMed: 12778124]
24. Amano M, Nakayama M, Kaibuchi K. Rho-kinase/ROCK: a key regulator of the cytoskeleton and cell polarity. Cytoskeleton (Hoboken). 2010; 67:545–554. [PubMed: 20803696]
25. Heikkila T, Wheatley E, Crighton D, Schroder E, Boakes A, Kaye SJ, et al. Co-crystal structures of inhibitors with MRCKbeta, a key regulator of tumor cell invasion. PLoS ONE. 2011; 6:e24825. [PubMed: 21949762]
26. Ito M, Nakano T, Erdodi F, Hartshorne DJ. Myosin phosphatase: structure, regulation and function. Mol. Cell. Biochem. 2004; 259:197–209. [PubMed: 15124925]
27. Yoneda A, Multhaupt HA, Couchman JR. The Rho kinases I and II regulate different aspects of myosin II activity. J. Cell Biol. 2005; 170:443–453. [PubMed: 16043513]
28. Liao JK, Seto M, Noma K. Rho kinase (ROCK) inhibitors. Cardiovasc. J. Pharmacol. 2007; 50:17–24.
29. Hahmann C, Schroeter T. Rho-kinase inhibitors as therapeutics: from pan inhibition to isoform selectivity. Cell. Mol. Life Sci. 2010; 67:171–177. [PubMed: 19907920]
30. Pan P, Shen M, Yu H, Li Y, Li D, Hou T. Advances in the development of Rho-associated protein kinase (ROCK) inhibitors. Drug Discov. Today. 2013; 18:1323–1333. [PubMed: 24076262]
31. Leung T, Chen XQ, Manser E, Lim L. The p160 RhoA-binding kinase ROK alpha is a member of a kinase family and is involved in the reorganization of the cytoskeleton. Mol. Cell. Biol. 1996; 16:5313–5327. [PubMed: 8816443]
32. Katoh K, Kano Y, Ookawara S. Rho-kinase dependent organization of stress fibers and focal adhesions in cultured fibroblasts. Genes Cells. 2007; 12:623–638. [PubMed: 17535253]
33. Routhier A, Astuccio M, Lahey D, Monfredo N, Johnson A, Callahan W, et al. Pharmacological inhibition of Rho-kinase signaling with Y-27632 blocks melanoma tumor growth. Oncol. Rep. 2010; 23:861–867. [PubMed: 20127030]
34. Somlyo AV, Bradshaw D, Ramos S, Murphy C, Myers CE, Somlyo AP. Rho-kinase inhibitor retards migration and in vivo dissemination of human prostate cancer cells. Biochem. Biophys. Res. Commun. 2000; 269:652–659. [PubMed: 10720471]
35. Imamura F, Mukai M, Ayaki M, Akedo H. Y-27632, an inhibitor of Rho-associated protein kinase, suppresses tumor cell invasion via regulation of focal adhesion and focal adhesion kinase. Jpn. J. Cancer Res. 2000; 91:811–816. [PubMed: 10965022]
36. Yang XY, Zhang Y, Wang SM, Shi WJ. Effect of fasudil on growth, adhesion, invasion, and migration of 95D lung carcinoma cells in vitro. Can. J. Physiol. Pharmacol. 2010; 88:874–879. [PubMed: 20921973]
37. Yang X, Di J, Zhang Y, Zhang S, Lu J, Liu J, et al. The Rho-kinase inhibitor inhibits proliferation and metastasis of small cell lung cancer. Biomed. Pharmacother. 2012; 66:221–227. [PubMed: 22425182]
38. Ying H, Biroc SL, Li WW, Alicke B, Xuan JA, Pagila R, et al. The Rho kinase inhibitor fasudil inhibits tumor progression in human and rat tumor models. Mol. Cancer Ther. 2006; 5:2158–2164. [PubMed: 16985048]
39. Patel RA, Forinash KD, Pireddu R, Sun Y, Sun N, Martin MP, et al. RKI-1447 is a potent inhibitor of the Rho-associated ROCK kinases with anti-invasive and antitumor activities in breast cancer. Cancer Res. 2012; 72:5025–5034. [PubMed: 22846914]
40. Nakajima M, Hayashi K, Egi Y, Katayama K-I, Amano Y, Uehata M, et al. Effect of Wf-536, a novel ROCK inhibitor, against metastasis of B16 melanoma. Cancer Chemother. Pharmacol. 2003; 52:319–324. [PubMed: 12783205]

41. Gaggioli C, Hooper S, Hidalgo-Carcedo C, Grosse R, Marshall JF, Harrington K, et al. Fibroblast-led collective invasion of carcinoma cells with differing roles for RhoGTPases in leading and following cells. Nat. Cell Biol. 2007; 9:1392–1400. [PubMed: 18037882]

42. Fritz G, Just I, Kaina B. Rho GTPases are over-expressed in human tumors. Int. J. Cancer. 1999; 81:682. [PubMed: 10328216]

43. Fritz G, Brachetti C, Bahlmann F, Schmidt M, Kaina B. Rho GTPases in human breast tumours: expression and mutation analyses and correlation with clinical parameters. Br. J. Cancer. 2002; 87:635–644. [PubMed: 12237774]

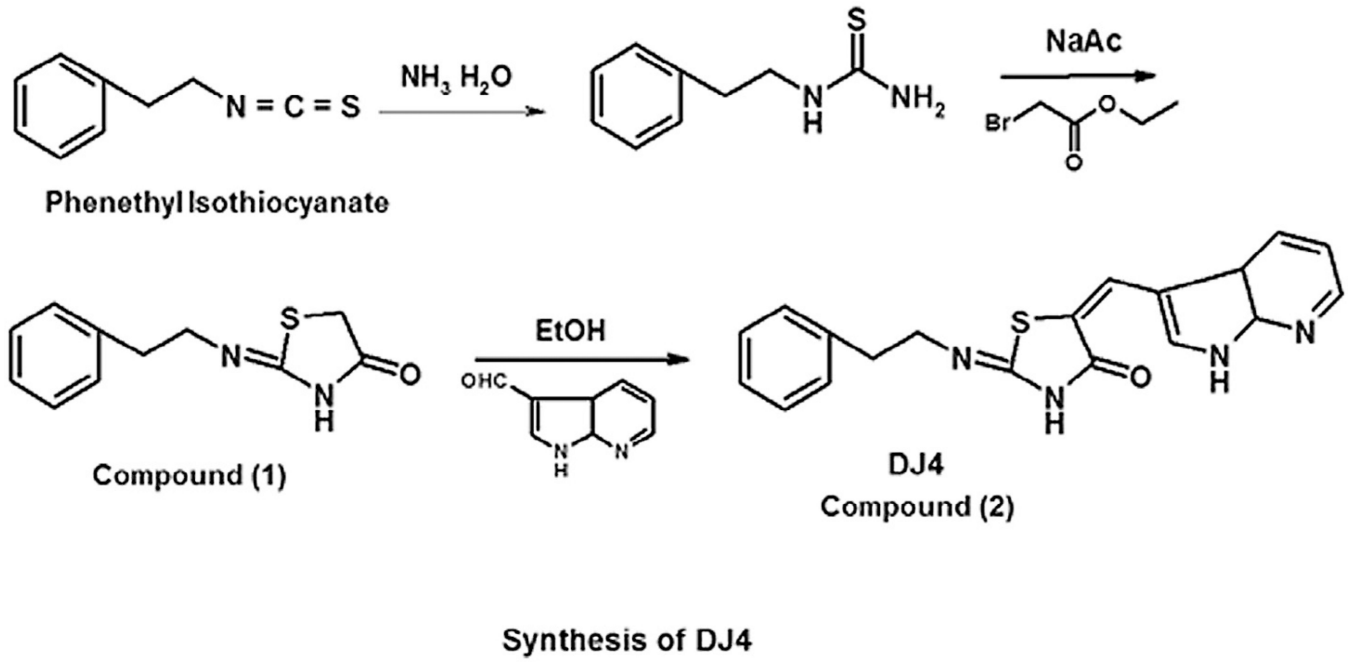

Fig. 1.
Chemical synthesis and structure of DJ4.

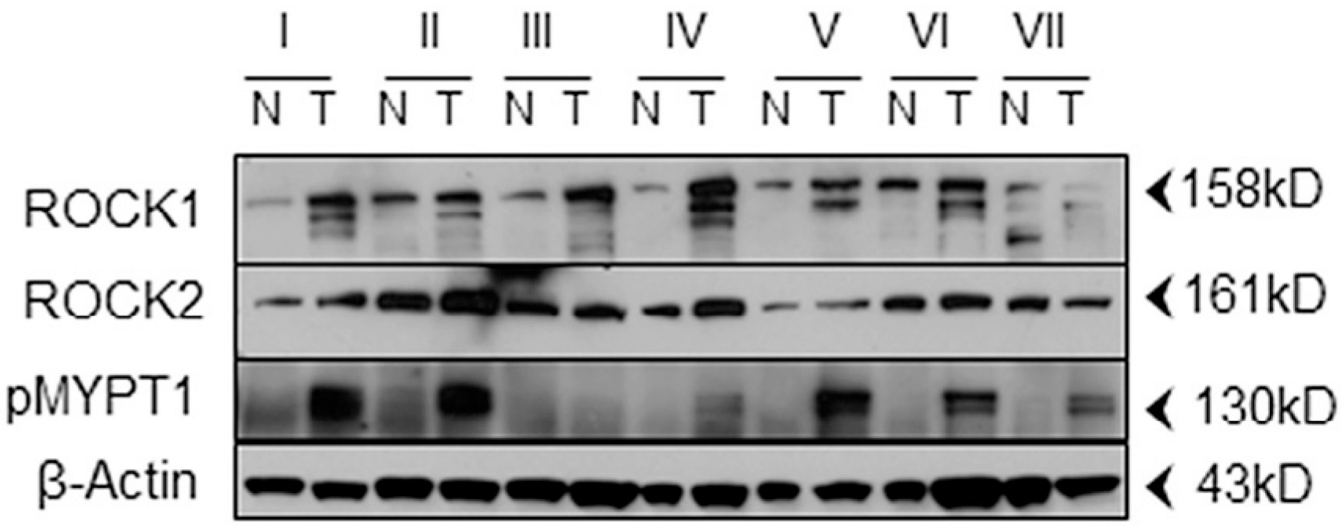

Fig. 2.

ROCK1, ROCK2 and/or pMYPT1 are overexpressed in human metastatic lung cancers. Patient matched paired normal (N) and tumorous (T) lung tissues were obtained and the expression patterns of the indicated proteins were determined by Western blot analysis. Roman numerals indicate patient samples as follows: I, squamous cell carcinoma; II, metastatic carcinoma of breast origin; III, metastatic sarcoma; IV, metastatic adenocarcinoma of endometrial origin; V, carcinoma; VI, metastatic pleomorphic sarcoma; VII, squamous cell carcinoma.

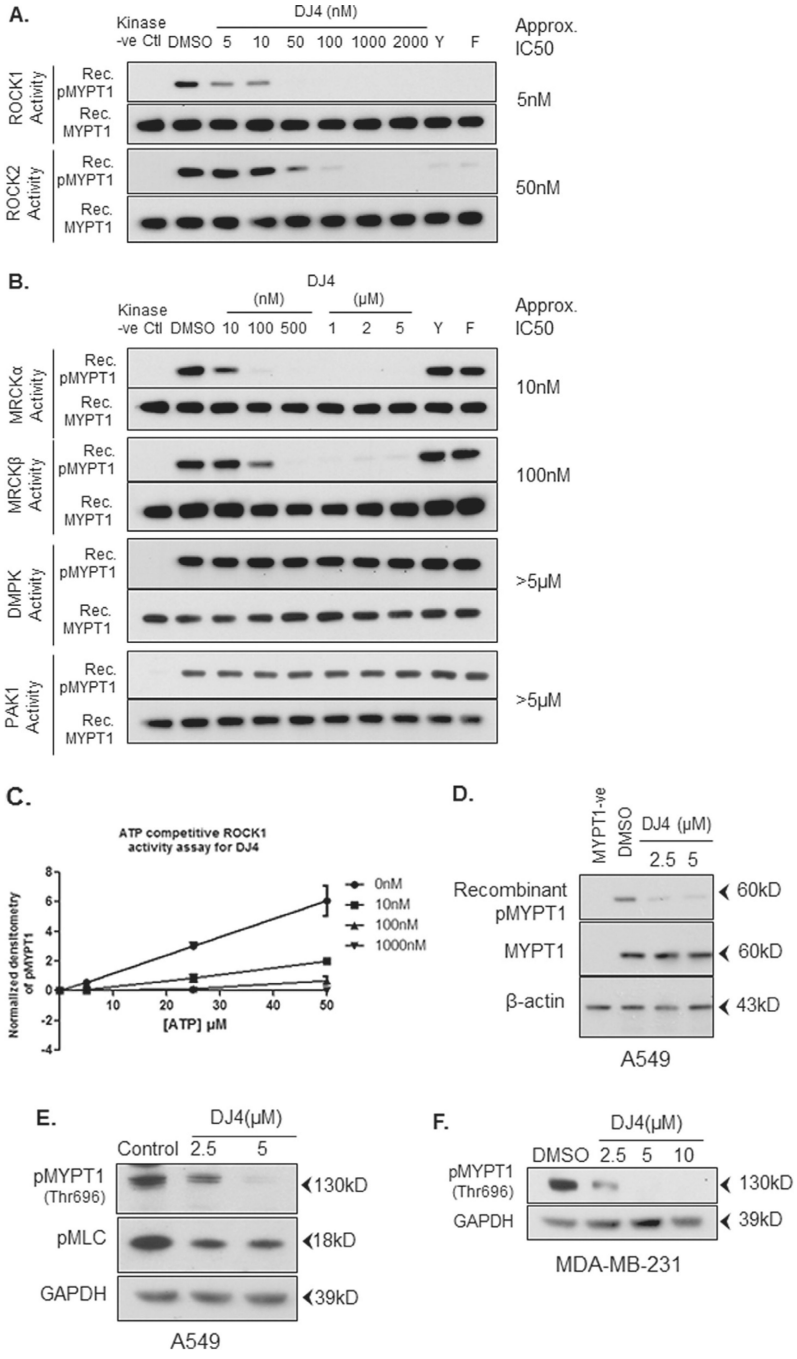

Fig. 3.

DJ4 selectively inhibits ROCK and MRCK over PAK1 or DMPK. (A and B) Recombinant proteins were incubated in the presence of MYPT1 peptide substrate, ATP (5 μM) and either DMSO or DJ4, Y27632 (Y) or hydroxyfasudil (F). Known ROCK inhibitors Y27632 and hydroxyfasudil (both at 1 μM) were used as positive controls. Samples without respective kinases were used as negative controls. Phosphorylation of the MYPT1 peptide substrate was detected by Western blot analysis using antibodies specific for phospho-Thr696 of MYPT1. Total MYPT1 (anti-MYPT1) was used as a loading control (C). DJ4 (10, 100 and

1000 nM) inhibits ROCK1 activity in an ATP competitive manner (5, 25, 50 μM ATP). (D) A549 cells were treated with DJ4 or DMSO for 24 h. Equal amounts of total protein lysates were incubated with recombinant MYPT1 peptide substrate in the presence of ATP (25 μM). Phosphorylation of the MYPT1 peptide substrate was detected by Western blot analysis using antibodies specific for phospho-Thr696 of MYPT1. Cell lysate without recombinant MYPT1 was used as negative control. (E) A549 cells were treated with either DMSO or the indicated concentration of DJ4 for 24 h. Endogenous phosphorylation of MYPT1 and MLC was detected using antibodies specific for phospho-Thr696 of MYPT1 and phospho-Ser19 of MLC. (F) MDA-MB-231 breast cancer cells were treated with indicated concentrations of DJ4 for 24 h and Western blot analysis was performed for endogenous pMYPT1(Thr696). GAPDH was used as a loading control.

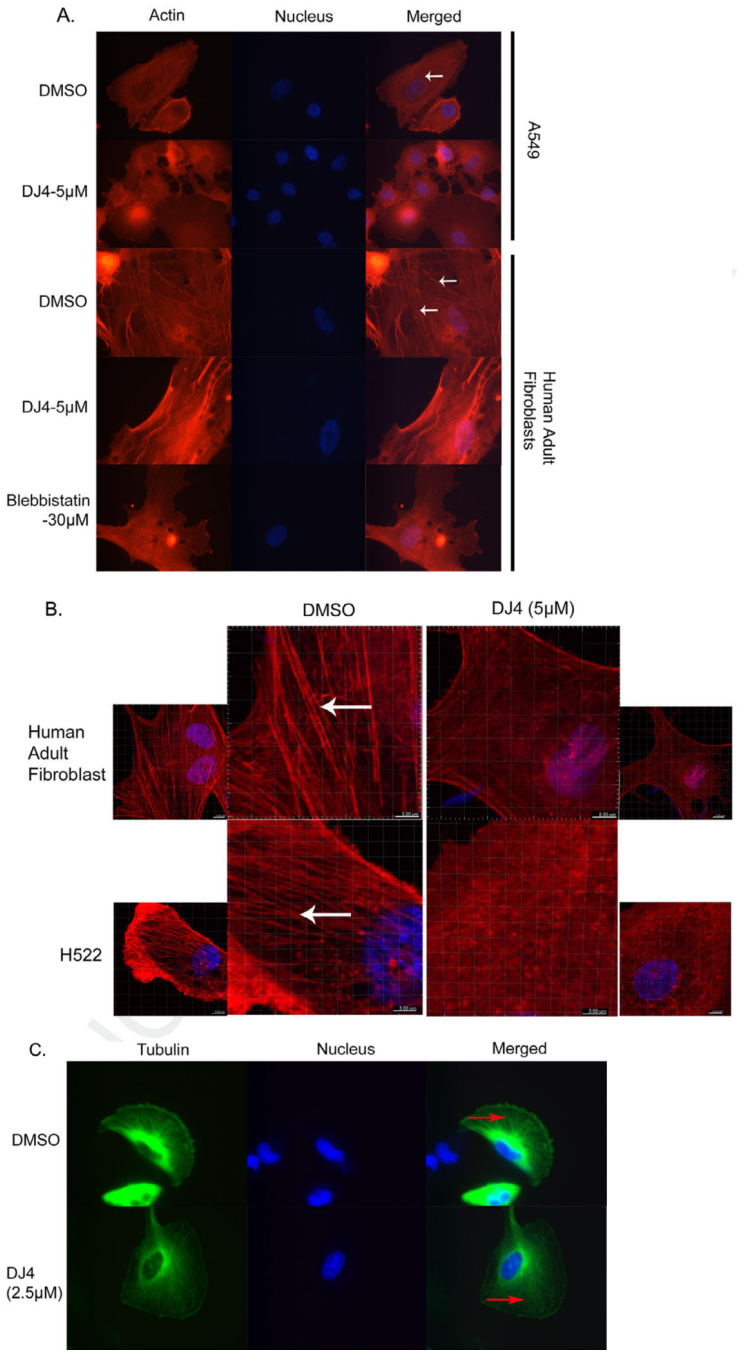

Fig. 4.

Cytoskeletal changes induced by DJ4 in A549, H522, U251 and human adult fibroblast cells after DJ4. (A) A549 and fibroblasts were treated with DJ4 for 1 h and stained with rhodamine-phalloidin and DAPI for visualization of stress fibers (red; indicated by white arrow) and nuclei (blue) respectively. Images were captured at 600× magnification using an inverted fluorescent microscope with an oil objective. (B) Normal human adult fibroblasts and H522 cells were treated with 5 μM DJ4 for 8 h and 3.5 h respectively. Cells were stained for stress fibers (red colored indicated by white arrow) with rhodamine-phalloidin

and for nuclei (blue) with DAPI. Images were captured at 400× under a confocal microscope. (C) U251 glioblastoma cells stably expressing EGFP-Tubulin were treated with DMSO or DJ-4 (2.5 μM) for 4 h, fixed and nuclei were stained with DAPI. Red arrows indicate microtubules (green). Images were captured at 600× using an inverted fluorescent microscope with an oil objective. (For interpretation of the references to color in this figure legend, the reader is referred to the web version of this article.)

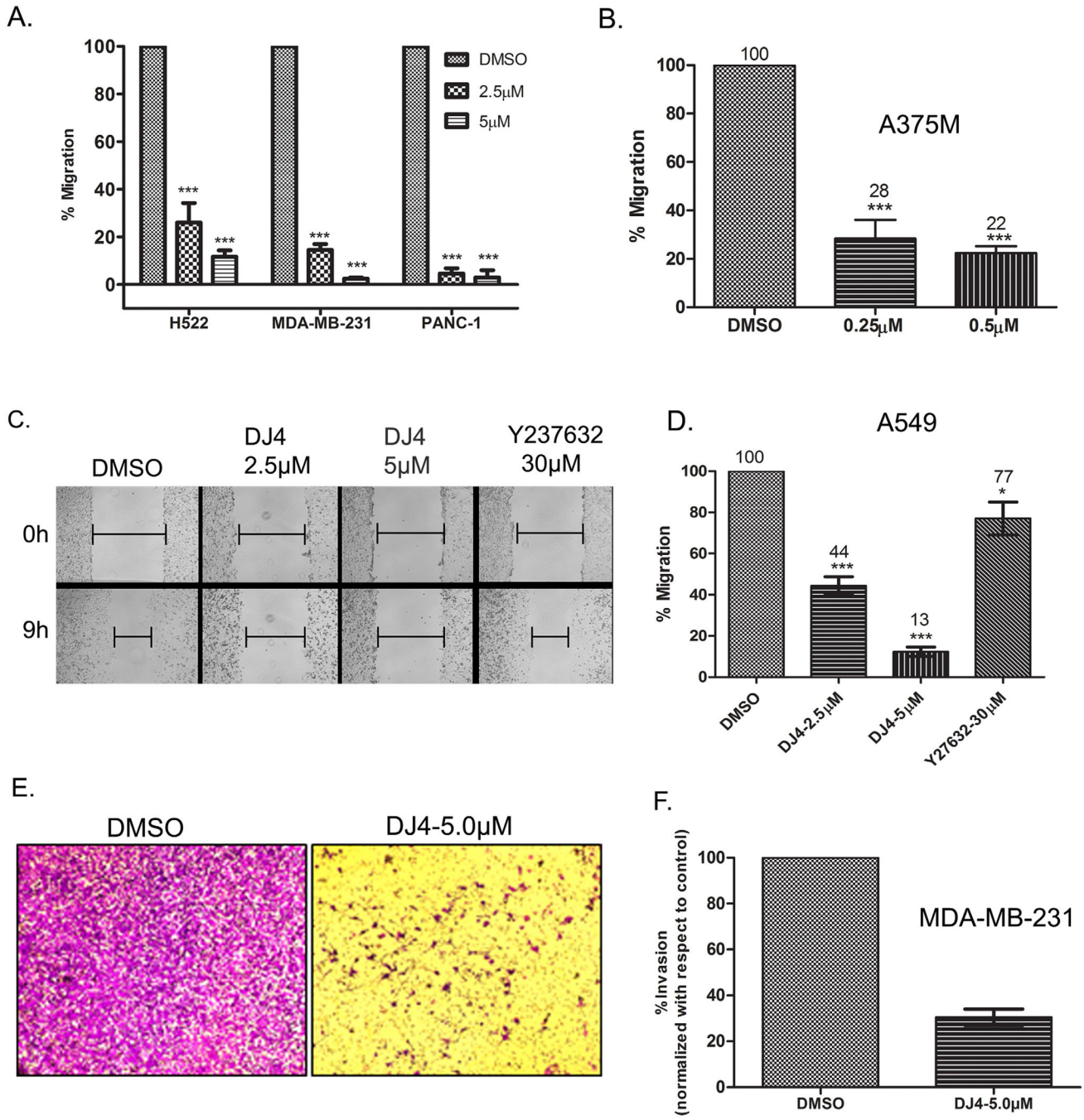

Fig. 5.

DJ4 inhibits migration and invasion of cancer cells. (A and B) Percent migration relative to control treated cells was determined by performing scratch assays in (A) lung adenocarcinoma (H522), breast (MDA-MB-231), pancreatic (PANC-1) and (B) melanoma (A375M) cancer cell lines. Cells were treated with DJ4 or DMSO for 24 h then monolayers were wounded and migration was allowed to proceed for 6–7 h (MDA-MB-231 and PANC-1) and 11–12 h (A375M) in the presence of DJ4 or DMSO. Error bars indicate SEM (n = 3, except for MDA-MB-231 where n = 2). ***P < 0.0001. (C and D) A549 cells treated

with DJ4, Y-27632 or DMSO for 24 h. Monolayers were then wounded and migration was allowed to proceed for 9 h in treatment-free medium (C). Percent migration relative to control treated cells was determined and quantitative analysis of migration of A549 cells is presented in (D). (E and F) MDA-MB-231 cells were treated with DMSO or the indicated concentrations of DJ4 and allowed to invade through Matrigel coated membranes (8.0 μm) for 48 h. The error bars indicate SEM from two independent experiments.

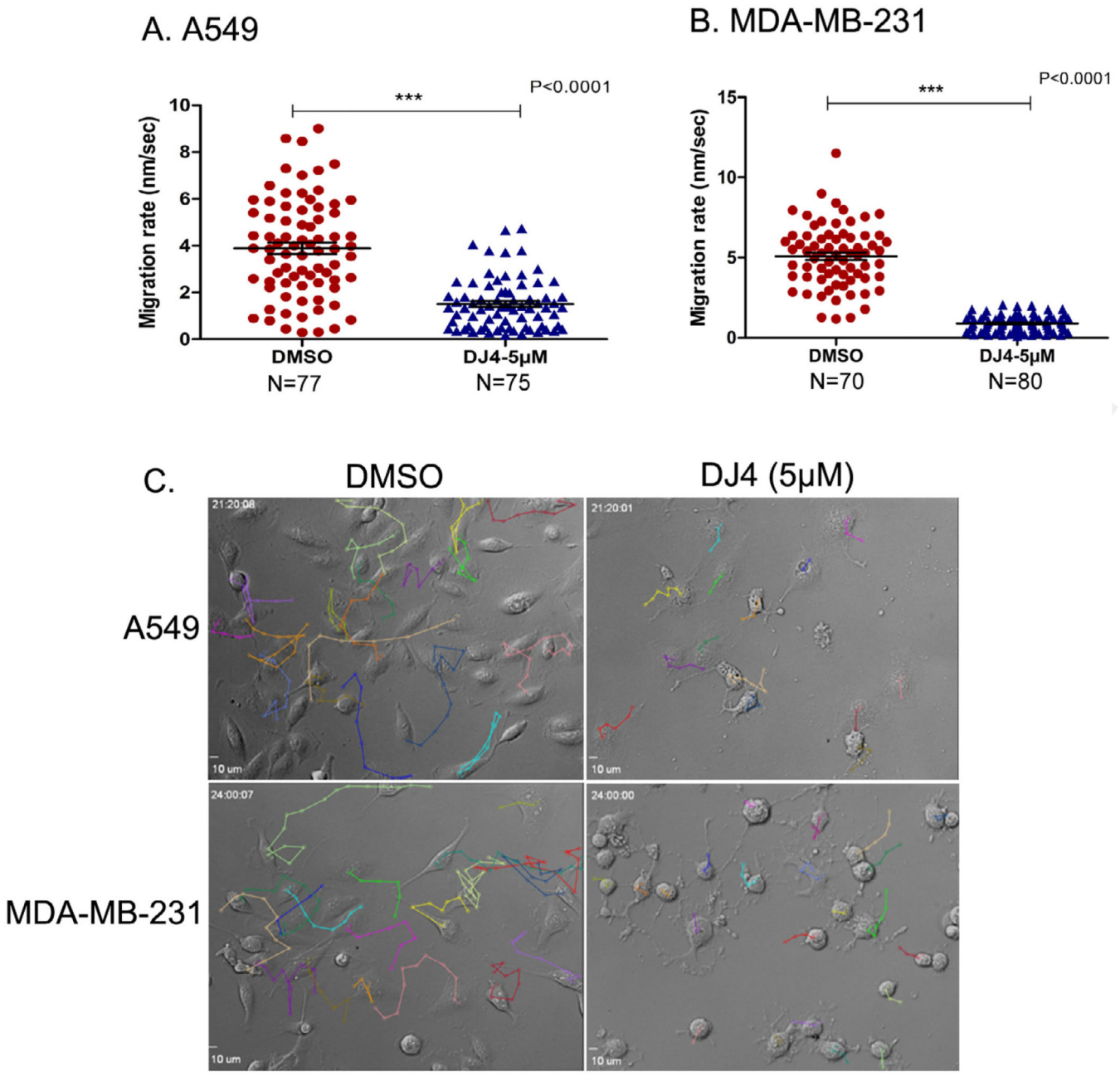

Fig. 6.

Single cell tracking of lung and breast cancer cells. (A and B) Scatter plots representing the migration rate of A549 cells (A) and MDA-MB-231 cells (B) (from four fields) treated with either DJ4 (5 μM) or DMSO (vehicle control). Error bars indicate SEM. (C) Individual cells from representative fields of A549 and MDA-MB-231 cells treated with either DMSO or DJ4 that were tracked to determine migration rate over a 21–24 h period.

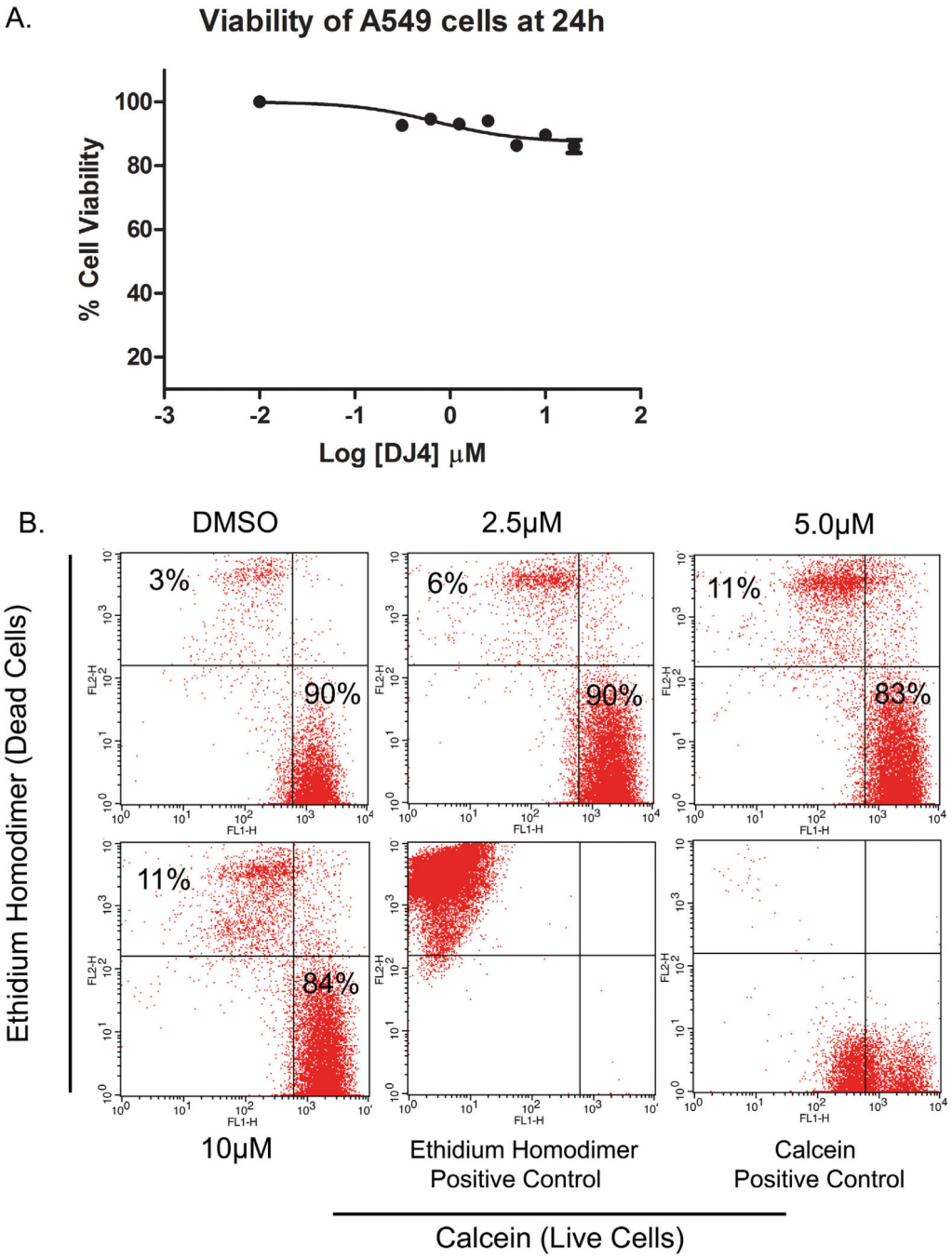

Fig. 7.

Inhibition of cell migration by DJ4 is independent of cell death induction. (A) A549 cells were treated with various concentration of DJ4 for 24 h. Cells were further incubated with MTT and formazan crystals were dissolved in DMSO. Color intensity was measured by spectrophotometer. Cell viability of DJ4 treated cells was determined relative to vehicle treated controls. (B) A549 cells were treated for 24 h and stained with calcein and ethidium-homodimer. Live (calcein positive) and dead cells (ethidium-homodimer) were counted by flow cytometry.

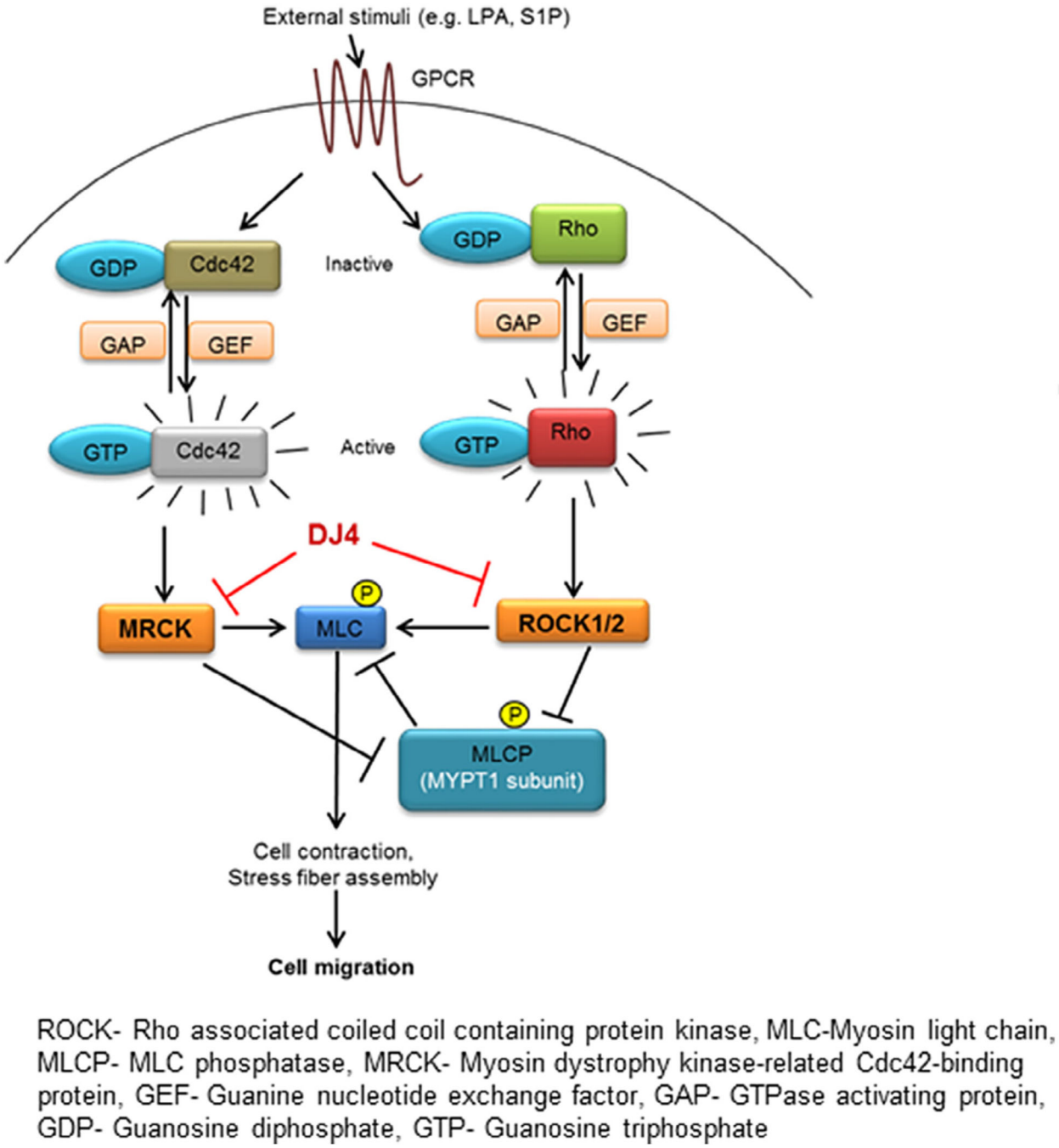

Fig. 8.

Schematic representation of the effects of DJ4 on migration/invasion. Ligation of G-protein coupled receptors activates Rho and Cdc42 signaling to activate ROCK1/2 and MRCKα/β, respectively, resulting in formation/contraction of stress fibers and cellular migration. DJ4 through inhibition of ROCK1/2 and MRCKα/β blocks the phosphorylation of MLC at Ser19 resulting in disruption of stress fiber formation. Simultaneously, by inhibiting ROCK1/2 and MRCKα/β activity, DJ4 also blocks the inactivating phosphorylation of MYPT1 (Thr696), the regulatory subunit of myosin light chain phosphatase (MLCP) resulting in the activation

of MLCP. Active MLCP further enforces the dephosphorylated state of MLC at Ser19. Thus the DJ4 mediated disruption of stress fiber formation inhibits cellular migration/invasion.